HOSTED BY

ELSEVIER

Contents lists available at ScienceDirect

Saudi Journal of Biological Sciences

journal homepage: www.sciencedirect.com

الجمعية السعودية لعلوم الحياة
SAUDI BIOLOGICAL SOCIETY

Original article

A novel approach to insulin delivery via oral route: Milk fat globule membrane derived liposomes as a delivery vehicle

Shaheer Shafiq [a], Maisa Siddiq Abduh [b,c], Fareeha Iqbal [a], Kousain Kousar [a], Sadia Anjum [d], Tahir Ahmad [a,*]

[a] Atta-Ur-Rahman School of Applied Biosciences, National University of Sciences and Technology (NUST), Islamabad, Pakistan
[b] Immune Responses in Different Diseases Research Group, Department of Medical Laboratory Sciences, Faculty of Applied Medical Sciences, King Abdulaziz University, Jeddah, Saudi Arabia
[c] Center of Excellence in Genomic Medicine Research, King Abdulaziz University, Jeddah, Saudi Arabia
[d] Department of Biology, University of Hail, Saudi Arabia

ARTICLE INFO

Keywords:
Camel milk
MFGM
Liposomes
Insulin
Diabetes
Streptozotocin

ABSTRACT

The current research endeavor seeks to unlock the potential of orally administered insulin formulations by utilizing liposomes derived from the fat globule membrane (MFGM) of camel milk as carriers for insulin. This pursuit emerges as a result of the recognized limitations of subcutaneous insulin therapy. The liposomes were meticulously created using the thin film hydration method, followed by comprehensive chemical and morphological analyses. Additionally, comprehensive safety assessments were carried out *in vitro* and *in vivo*, revealing significant findings.

The Fourier-transform infrared (FTIR) spectrum confirmed the presence of insulin within the liposomes, demonstrating changes in their size and charge. The *in vitro* cytotoxicity analysis, performed on HEK-293 cell lines through the MTT assay, yielded results indicating a cell viability of over 90%. In the *in vivo* investigation, diabetic rats induced by STZ were utilized to evaluate the effects of the liposomes, revealing substantial reductions in blood glucose levels, bilirubin, alkaline phosphatase (ALP), albumin, and alanine aminotransferase (ALT) levels. Hepatic histopathological assessments showed signs of recovery across all treatment groups, with no observable microscopic changes in renal tissue. This investigation highlights the significant hypoglycemic effects observed in insulin-loaded liposomes derived from MFGM obtained from camel milk when administered orally.

1. Introduction

Proteins and peptides, as well as other bioactive pharmacological compounds, are now being considered as potential therapeutic agents for the treatment of a range of diseases related to cancer, metabolic disorders, and urinary tract disorders (Aboonabi et al., 2014; Abud et al., 2019). Until now, the administration of peptides and proteins for protection against stomach acidity and inadequate bioavailability in the intestinal epithelium has been accomplished solely through the parenteral route, which involves intravenous infusions (Aboonabi et al., 2014; Abud et al., 2019; Ali et al., 2019; Anwar et al., 2021). Diabetic patients often rely on subcutaneously administered exogenous insulin peptides to manage their condition, but this approach has numerous drawbacks. Patients frequently experience physical discomfort, pain, and injection inconvenience, as well as erythema, hematoma, and lipodystrophy at the injection site, including lipoatrophy and lipo-hypertrophy. Additionally, patients may suffer from allergic reactions, hypoglycemia due to repeated intramuscular injections, hyperinsulinemia, and weight gain, all of which compromise patient compliance (Aboonabi et al., 2014; Ali et al., 2019).

The administration of insulin peptide via non-parenteral means has proven to be a formidable challenge in contemporary pharmacological research. The utilization of buccal, nasal, and pulmonary routes poses significant challenges, with the oral route being particularly problematic. However, this route presents a viable alternative to parenteral administration and offers a practical solution to the issue of high patient

* Corresponding author at: Atta-Ur-Rahman School of Applied Biosciences, National University of Sciences and Technology (NUST), Islamabad, Pakistan.
E-mail addresses: sshafiq.msib08asab@student.nust.edu.pk (S. Shafiq), mabdoh@kau.edu.sa (M. Siddiq Abduh), fiqbal.msib08asab@student.nust.edu.pk (F. Iqbal), kkousar.phdabsa9asab@student.nust.edu.pk (K. Kousar), s.anjum@uoh.edu.sa (S. Anjum), tahir@asab.nust.edu.pk (T. Ahmad).

https://doi.org/10.1016/j.sjbs.2024.103945
Received 20 July 2023; Received in revised form 24 January 2024; Accepted 26 January 2024
Available online 28 January 2024

compliance. It is also a safe and prompt method for insulin delivery (Aqib et al., 2019). The bioavailability of oral insulin has been reduced due to the presence of gastric and proteolytic degradation in the GI tract, together with poor permeability of insulin peptides within the gut epithelia (Abud et al., 2019; Anwar et al., 2021; Aqib et al., 2019). The aforementioned problems sparked by insulin therapy call for substitute techniques for insulin administration.

A number of strategies have been developed over the last few years in order to cope with possible drawbacks related to administering insulin orally, including coadministration of insulin with absorption enhancers, enzyme inhibitors, increased lipophilicity and permeability by chemical modifications, and nanoencapsulation of insulin into nanocarriers has emerged as a novel approach (Arranz, 2017; Ayoub et al., 2018). Encapsulation of insulin within liposomes is considered to be a viable method for overcoming the limitations associated with conventional insulin therapy that is currently administered orally (Anwar et al., 2021; Bakry et al., 2021; Balamash et al., 2018).

Liposomes, which are closed vesicles formed by a self-assembled bilayer of lipids, have exhibited enhanced pharmacodynamic and pharmacokinetic properties as well as heightened bioavailability of cargo when administered orally (Abud et al., 2019; Ali et al., 2019; Chai et al., 2022; Clogston and Patri, 2011), tending to protect the cargo and impede its degradation in simulated intestinal fluid (SIF) and simulated gastric fluid (SGF) (Anwar et al., 2021; Balamash et al., 2018; Contarini and Povolo, 2013). Liposomes can be formed either from synthetic or natural phospholipids such as egg yolk, and soybean phospholipids use for oral delivery of insulin (Ali et al., 2019; Evers et al., 2008; Hameed et al., 2023; He et al., 2018) and one of the natural sources is milk phospholipids (Ibišević et al., 2019). One of the milk sources is camel, and research has shown that camel milk has anti-diabetic, anti-HCV, anti-inflammatory, and anti-cancerous characteristics (Clogston and Patri, 2011; Ismail et al., 2018; Izadi and Khedmat, 2019; Jabs, 2005). Furthermore, it was observed that the administration of camel milk to animals with induced diabetes resulted in an amelioration of glucose levels in the bloodstream, as well as enhancements in serum insulin and lipid profiles. This benefit is linked to the large number of insulins like protein and insulin components present in camel milk, which has been associated with a strengthening of receptor function related to insulin (Jash, 2022; Jash et al., 2020; Lee et al., 2018; Liu et al., 2013).

Insulin, entrapped in camel milk, contains distinct characteristics which cause hindrance to protein degradation, making adsorption easier into the circulation when compared with insulin that is derived from different sources other than camel milk (Jabs, 2005; Lee et al., 2018; Liu et al., 2020). Within camel milk, a total of 3% of fats present are identified to possess antidiabetic potential (Izadi and Khedmat, 2019; Malik et al., 2012). In the aqueous phase of milk, the fat molecules are observed to be present as globules that are emulsified and stabilized by a complex membrane structure known as MFGM (milk fat globule membrane) (Clogston and Patri, 2011; Malik et al., 2015). The Multi-Layered Fat Globule Membrane (MFGM) is comprised of a trilaminate structure, with the initial layer being predominantly populated with proteins, which encase the neutral lipids that are located intracellularly (He et al., 2018; Maswadeh et al., 2015; Matteucci et al., 2015).

Camel milk possess phospholipids that have antidiabetic, antioxidant and angiotensin-I-converting enzyme (ACE) inhibitory enzyme that possess the anti-hypertensive potential (Jabs, 2005). The composition of MFGM in camel milk unveils the phospholipid percentage to be 26 % (Malik et al., 2012), these phospholipids can be extracted from MFGM for molding them into liposomes as these liposomes possess the ability to protect the bioactive compound's functional and nutritional characteristics (Clogston and Patri, 2011; Mirmiran et al., 2017; Nagarchi et al., 2015). Considering this aspect, insulin can be encapsulated inside MFGM liposomes for targeting diabetes mellitus (Nguyen et al., 2014). To the best of our knowledge, the capability of camel milk MFGM-based liposomes as an oral insulin delivery system has not been investigated yet, despite its holding immense anti-diabetic potential. Thereupon, this study intended to manifest the potential of camel milk based MFGM liposomes encasing insulin as cargo for oval delivery which would address the shortcomings associated with conventional insulin therapy, followed by its characterization and *in vitro* and *in vivo* safety analyses.

2. Material and method

2.1. Chemicals

Streptozotocin (STZ), Phosphate buffer saline (PBS), chloroform, methanol, fructose, Sodium chloride (NaCl), Dimethyl Sulfoxide (DMSO), Formalin, Paraffin Wax, Ethanol, Xylene, Glycerin, Hematoxylin, Eosin, DPPX and MTT (3-(4,5-Dimethylthiazole-2-yl) were purchased from Sigma Aldrich (USA) by Bio-life Technologies through Science Home Traders. Cell culture media Dulbecco's Modified Eagle Medium (DMEM), Fetal Bovine Serum (FBS), and Pen-Strap (10,000 U/mL Penicillin, 10 µg/mL Streptomycin) were purchased from Gibco through Bio-life technologies Islamabad, Pakistan. For biochemical analyses, diagnostic kits were purchased from Bio Research and CHEMELEX S.A Diagnostic reagents. Mixtard 30/70 insulin injections were purchased from the D. Watson chemists, Islamabad, Pakistan. All the above-mentioned chemicals are analytically graded and used without further purification.

2.2. Formulation of MFGM-derived insulin loaded liposomes

2.2.1. Camel milk collection

Camel milk was procured from two prevalent species, *Brella* and *Marecha*, from a local market in Islamabad, Pakistan. A single batch of one-liter fresh milk was obtained and swiftly placed in sanitized plastic containers, which were then transferred to a laboratory in temperature-controlled ice box. For later use, the samples were kept in sterilized bottles at 4°C.

2.2.2. Extraction of milk fat globule membrane (MFGM)

Camel milk MFGM extraction was carried out by the process performed by P. Malik et al. (2015) (Niu et al., 2012) with slight modifications, briefly explained, The process began with boiling the camel milk, followed by cooling it to room temperature. The cream layer, which formed on the surface, was separated, and stored at 4℃ in 50 ml falcon tubes for further use. Subsequently, the cream was washed thrice with Phosphate Buffer Saline soln. (1M) by centrifuged at 5500 rpm for ten minutes at 4℃. The cream was subjected to a process of emulsification and thermal treatment in a water bath maintained at a temperature of 45°C for a period of thirty minutes, following a storage period of twenty hours at 4°C. The next day, serum phase was then collected by filtering with filter cloth, and the process repeated thrice. After the collection of serum, the material was subjected to centrifugation at a speed of 6000 revolutions per minute (rpm) for a duration of 15 min at a temperature of 4°C. At that stage, the resulting liquid serum phase was recovered and maintained at a temperature of −20°C to be ready for subsequent processing. The frozen sample (Liquid Serum phase) was transferred to the freeze-drying chamber. After subjecting MFGM to the freeze-drying process for a duration of 24h at a temperature of −56°C and a pressure of 0.1 mbar, the resultant form of the product was obtained in its desiccated state. The Freeze-drying process was done at the Bioprocess laboratory of Atta-Ur-Rahman School of Applied Biosciences (ASAB) at the National University of Sciences and Technology (NUST).

2.2.3. Extraction of lipids from MFGM

For lipid extraction, 1g dried sample of MFGM washed with a 2:1 chloroform/methanol solution (30 ml) and manually shaken for 10 min. The resultant solution was centrifuged at 3000 rpm, and after each of the three wash cycles, the supernatant was filtered using a 5µm filter sheet in a separation flask. Following this, 40 ml of 0.57 % sodium chloride solution was added to the separation funnel and allowed to stand

overnight. The organic layer was separated from the separating funnel, 20 ml of chloroform was added in it, and it was let to stand for 3–4 h. Finally, the solvent from the organic layer was collected and evaporated by using a rotary evaporator, resulting in the remaining sample being lipids.

2.2.4. Preparation of liposomes and insulin loading

After carefully collecting the lipids with 10ml of 2:1 chloroform/ethanol solution, a thin film was produced by employing a rotary evaporator for one hour at 50°C in a round bottom flask. The flask was left to stand at room temperature for two hours following the thin film formation. Proceeding this, 1 ml of insulin was added to a 10ml solution of liposomes and PBS to rehydrate the thin film. The rehydrated solution was centrifuged at 6000 rpm for 15 mins and the pellet was collected and redispersed in 10ml PBS solution. The liposomes were viewed under the light microscope and were then again centrifuged at 6000 rpm for 15 mins. The collected pellet was obtained and kept in the refrigerator at 4°C for further use (Clogston and Patri, 2011).

2.3. Characterization of MFGM derived insulin-loaded liposomes

To ascertain the formation of the encapsulation and their overall topography, a series of chemical and morphological characterization tests on the liposomes loaded with insulin were performed.

2.3.1. Optical imaging

On the glass slides, a small number of liposomes was put, and the coverslips were angled to prevent bubble forming. After placing the coverslip, the slide was observed under a microscope at 40X and the image was taken using Optika ProView software (Niu M,Tan Yn, Guan P, Hovgaard L, Lu Y, Qi J, 2014).

2.3.2. Insulin encapsulation efficiency

The efficiency of liposomes for encapsulating insulin was assessed by UV–vis spectroscopy (A&E Lab, UV Visible Spectrophotometer, AE-S90) at 320 nm. The concentration of insulin was determined using a calibration curve based on wavelength, which was generated using the Claw. Before analysis, the formulations were centrifuged at 6000 rpm for 15 min to remove the unencapsulated insulin. The difference between the total insulin added into the system and that of the supernatant unencapsulated insulin was used to determine the encapsulation efficiency percentage.

$$\text{EE\%} = \frac{\text{Total amount of drug} - \text{unbound drug in supernatant}}{\text{Total amount of drug}} \times 100$$

2.3.3. Release profile

The insulin-loaded liposomes are placed in a tube, to which 2ml phosphate buffer (pH 7.4) is added as the release medium for simulating physiological conditions. The tubes are then immersed in a water bath by placing on a horizontal shaker at a constant 37 ± 0.5°C to ensure even distribution of the liposomes. At predetermined time intervals, 1.5ml samples are withdrawn and immediately replaced with fresh medium to maintain constant conditions. These samples are further centrifuged at 6000 rpm for 15 min, effectively separating the released insulin in the supernatant from the liposome. The concentration of insulin in the supernatant is quantified using the Lamber-Beer method, involving monitoring absorption at 320nm. The data collected from these measurements are plotted against time to construct the release profile of insulin from the liposomes. This comprehensive methodology ensures a thorough understanding of the release profile of insulin-loaded liposomes, crucial for evaluating their potential in insulin therapy.

2.3.4. Release kinetics modeling

The kinetic analysis of the *in vitro* release data for insulin-loaded liposomes was conducted using the DD Solver program. This approach was employed to characterize the drug release kinetics and to ascertain the release mechanism of the insulin from the liposomal formulations. The release data obtained from the experimental studies was fitted to various kinetic models, including Zero Order, First Order, Higuchi's model, and the Korsmeyer-Peppas model. The equations for these models are as follows:

Zero order equation

$$Qt = Q0 + K0t$$

where Q0 is the initial amount of drug in the solution, Qt is the amount of drug released over time t and K0 is the zero-order rate constant.

First order rate equation:

$$logC = logC0 - Kt/2.303$$

In which K is the release constant of first order, t is time, and C0 is the starting concentration of the drug.

Higuchi's model:

$$Q = KHt.1/2$$

In which KH denotes dissolving constant of Higuchi model and Q denotes the quantity of drug released per unit area in time t.

Korsmeyer-peppas model:

$$\frac{Mt}{M\infty} = Kt^n$$

where K is the release rate constant, n is the release exponent, $\frac{Mt}{M\infty}$ represents the fraction of drug released at time t, and n indicates the mechanism of drug release.

2.3.5. Scanning electron microscope (SEM)

SEM (JSM-6490A) is used to determine the morphology and surface chemistry of an MFGM-derived liposome. Each sample was fixed overnight on a 6x6 mm slide using a 1:10 dilution. The following day, after mounting the dried samples onto a conducting surface attached to the glass slide via carbon tape, they were sputtered with gold. The slides were then inspected under a microscope at 15,000X and 20,000X magnification to determine the liposome's surface shape and size. The SEM facility was done at the Biomaterials laboratory of the School of Chemical and Material Engineering (SCME) at the National University of Sciences and Technology (NUST).

2.3.6. Attenuated total reflectance fourier transform infrared spectroscopy (ATR-FTIR)

For the detection of the interaction between the liposome and the insulin loaded into it, FTIR (Agilent ATR-FTIR, Spectrum 100), was performed between 450cm and 4500cm at room temperature. The absorbance and transmittance on different wavelength ranges help in the formation of a wave-like pattern that is unique to the respective bond and can help in identifying various drug bonds. At a resolution of $4^{cm\text{-}1}$ after 32 running scans, the spectra were collected. The FTIR facility was availed from the Biomaterials laboratory of the School of Chemical and Material Engineering (SCME) at the National University of Sciences and Technology (NUST).

2.3.7. Particle size and zeta potential determination

Using a Nano ZS zeta sizer and a Malvern device operating on the dynamic light scattering (DLS) principle, the particle size and zeta potential of insulin-loaded and blank liposomes were measured. The samples were redispersed in the PBS before the analysis and measurement was done at 25°C with a measurement position at 4.65 mm.

2.4. In vitro cytotoxicity evaluation of MFGM-derived insulin loaded liposomes

2.4.1. Cell line

To evaluate the cytotoxic effects of blank and insulin loaded MFGM derived liposomes, HEK-293 cells have been used. The cells of HEK-293 were obtained from ATCC Manassas, VA. In order to prevent bacterial contamination, HEK-293 had been grown in a moderate dose of DMEM culturing media that was enriched with 10% FBS and 0.5% Pen-Strep. The cells have been incubated at standard temperatures of 37°C, air temperature of 95% to 5% CO2, and humidity of 100%. Cells were used in the experiment for further examination while they were in the logarithmic phase of growth.

2.4.2. Cytotoxicity analysis

Cytotoxicity was assessed by using the MTT assay and by studying cell morphology changes in an inverted phase contrast microscope. The MTT dye [3-(4,5-dimethylthiazol-2-yl)-2,5-diphenyltetrazolium bromide] is analyzed based on the capacity of metabolically active/live cells to convert PBS-soluble formazan into an insoluble form (Nsairat et al., 2022). Cells were seeded in a flat bottom 96-well microtiter plate for 24h. After 1 day they were exposed to different concentrations (10 %, 40 %,70 %) of blank and insulin-loaded liposomes in triplicates and then incubated for 24h at standard conditions. Media was aspirated after 24h of incubation and cells were then incubated with 100 ml of medium containing 250 μg/mL MTT dye. After the addition of MTT dye, cells were incubated at 37°C for three hours in order to produce formazan particles. After dissolving the formazan particles in DMSO (20ul), the absorbance was assessed at 580 nm.

2.4.3. Cell morphology assay

In parallel with MTT experiment, cells have been studied by an inverted phase contrast microscope with 20X magnification, a digital sight camera and a digital imager. Morphological changes in cells were observed after they were treated with blank, and insulin-loaded liposomes.

2.4.4. Stability analysis

The stability of blank and Insulin-loaded liposomes was analyzed by observation of changes in the physical appearance of liposome suspension. Both blank and Insulin-loaded liposomes were stored at different temperatures of 25°C and 4°C for 48h followed by stability analysis. Zeta analysis results were analyzed to further confirm the stability of both forms of liposomes.

2.5. In vivo safety analysis of MFGM derived insulin loaded liposomes

2.5.1. Animals

The present experiment utilized female Wistar albino rats (n = 20) with ages ranging from 8 to 12 weeks and weighing between 197 and 242 g. The rats were housed in cages with a 12-hour light/dark cycle and maintained at a temperature of 25 °C. Throughout the experiment, the animals were provided with standard chow, which contained 23% of protein, 4% fibers, and 4–5% fats, and given fresh drinking water daily. Before the trial was started, rats spent a week acclimatizing themselves to laboratory conditions. These rats were procured from the Animal House facility of Atta-Ur-Rahman School of Applied Biosciences (ASAB) at the National University of Sciences and Technology (NUST) in Islamabad, Pakistan. All procedures involving animals were conducted in compliance with the ethical regulations of the Institutional Review Board (IRB) as denoted by the reference number IRB No. 11–2020-01/03. Additionally, the Laboratory Animal House (LAH) at ASAB, NUST, sanctioned and ensured the adherence to standard protocols.

2.5.2. Induction of diabetes

Streptozotocin (STZ) was dissolved in a 0.05M of citrate buffer (pH 4.5). Diabetes was Induced intraperitoneally with a single dose of Streptozotocin (40 mg/kg body weight) (Park et al., 2011). Instead of Streptozotocin, a non-diabetic control group (C) is injected with citrate buffer. Following Streptozotocin injections, rats were given ad. libitum 10% of (weight/volume) fructose solution and free access to standard meals for three consecutive days. In STZ treated rats, the development and stability of diabetes mellitus was permitted for more than 7 days. Diabetes mellitus was defined by measuring the blood glucose level by pricking the tail of a rat using a glucometer (On call Glucometer EZ II). The blood glucose levels of 250–300 mg/dl are considered to be diabetic.

2.5.3. Experimental group

The experimental groups comprising four normal rats (n = 4) and sixteen rats (n = 16) that were diabetic. These rats were separated into five different groups, each consisting of four rats. The nature of each group taken in this study is group 1 is healthy control animals (C) chow with normal feed and water. Group 2 contains diabetic control rats (DC) chow with normal feed and water. Group 3 is insulin-treated (DI) diabetic rats treated for 3 days with market-available insulin, Humulin 70/30, 1U/100 g of the body weight of rats. Group 4 is diabetic rats injected with insulin-loaded liposomes subcutaneously (2U/100 g) (SCL) for 3 days. Group 5 consists of diabetic rats treated for 3 days orally (OL) with insulin-loaded liposomes (4U/100 g).

2.5.4. Body weight

Before the onset of diabetes, and during the first and last days of treatment, the body weights of rats were measured using a digital balance. The experimental rat's weights were recorded at the same time in the morning. The signs of abnormal body weight were recorded throughout the experiment.

2.5.5. Blood glucose

One Call® EZ II blood glucose monitoring system was used for the routine blood glucose testing. Before the treatment fasting blood glucose levels and after 4 h of the treatment blood glucose level of the rats were observed. Blood samples for glucose testing of rats were taken by pricking the tails.

2.5.6. Blood sampling

The experimental animals were fasted for 12h after the end of the experiment, water was not restricted. Blood samples were collected by direct heart puncture in clotting blood tubes and organs are stored in 10% formalin and stored at −80 °C for further analysis. Blood samples have been centrifuged at 4000 rpm for five minutes and serum separated and stored up to −20°C for biochemical analysis.

2.6. Biochemical analysis

2.6.1. Liver function test (LFT)

Alkaline phosphatase (ALP), Alanine aminotransferase (ALT), Albumin (Alb), and Bilirubin (Bill) were measured in serum using Alkaline Phosphatase (SL), DGKC, (CZ001), ALT/GPT (SL), UV IFCC, (CZ003), Albumin, BCG, (CS001) (Bioresearch diagnostic kits) and BILIRUBIN T&D-DMSO DMSO, Colorimetric (CHEMELEX S.A Diagnostic reagents, ref #30157). Measurements were taken according to the manufacturer's guidelines by using Chemistry Analyzer (CHEMREADER Smart-N SE250).

2.6.2. Renal function test (RFT)

Creatinine and uric acid were measured in serum using Creatinine (SL), KINETIC, (CS006), and Uric Acid (SL), URICASE-PAP (CS018) (Bioresearch diagnostic kits British Columbia), respectively. Measurements were taken according to the manufacturer's instructions by using Chemistry Analyzer (CHEMREADER Smart-N SE250).

2.6.3. Histopathology

From all study groups, organ samples (liver and kidney) were fixed in 10% formalin and embedded in paraffin wax blocks. About 5–7μm thick microtome sections were cut, and H&E dye was used to stain them on a glass slide. Light microscopy (Optika B-150) was used to examine the slides, and Optika Vision Lite 2.1 was used to capture images.

2.7. Statistical analysis

GraphPad Prism Version 8.0.1 software was used to analyze all the data. The important values for different groups have been established by using ONE-WAY-ANOVA and the significant value has been considered when p value is less than 0.05.

3. Results

3.1. Liposomes formation and encapsulation efficiency

When a thin film is made and insulin solution is used to rehydrate it, it gives a white milky appearance. The solution is then washed with the phosphate buffer saline (PBS) and liposomes were settled at the bottom of the falcon tube as a milky pellet and a translucent milky solution with debris as the supernatant. Fig. 1 showed the pellet and supernatant of the liposomes loaded with insulin along with the thin film. To ensure that a therapeutic dose of insulin is encapsulated within the MFGM-derived liposomes, the entrapment efficiency is calculated. Insulin encapsulation efficiency in the liposomes was found 34 % and the calibration curve is presented in Fig. 2.

3.2. Optical microscopy

The multilamellar vesicles of the liposomes that were formed by the thin film hydration and loaded with insulin upon rehydration were observed immediately after formation by optical microscopy at 40X. It can also be observed that some of the liposomes can get agglomerate to form larger forms. Optical microscopic analysis images in Fig. 3 show the shape and morphology of the liposomes prepared from the camel milk derived MFGM and loaded with Insulin.

3.3. In vitro release profile

The *in vitro* insulin release from insulin-loaded liposomes over a 24-hour period was found to be approximately 77.44%. For the release profile, the linear model fitting yielded a correlation coefficient (R-squared) of 0.9045, as shown in Fig. 4.

3.4. Drug release kinetics

The high R^2 value for the zero order and korsmeyer-peppas models suggests these models fit the data well. The Korsmeyer-Peppas model, with n = 0.6055, indicates that the drug release mechanism is non-Fickian or anomalous, suggesting a combination of diffusion and erosion-controlled mechanisms. The values of the release kinetics of the insulin loaded liposomal formulations is given in Table 1 and cumulative release profile over a 24-hour period is mentioned in Fig. 5.

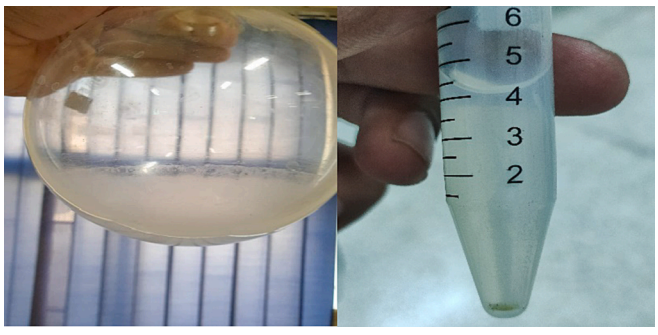

Fig. 1. Thin film formation in the round bottom flask and insulin-loaded liposomal pellet.

3.5. Physiochemical characterization of insulin loaded MFGM derived liposomes

3.5.1. Determination of functional groups by fourier transform infrared (FTIR) spectroscopy

To confirm the encapsulation of the insulin into the MFGM derived liposomes by predicting the functional groups of insulin Fourier Transform Infrared (FTIR) Spectra of the blank and insulin-loaded liposomes were observed. The obtained spectra are mentioned in Fig. 6. The spectra show a peak on 1634cm^{-1} and other peaks on 1552cm^{-1}, both of these peaks are characteristic peaks of the protein spectra and can be referred to as amide-I and amide-II, respectively. Both of these peaks compared to the blank liposome spectra represent the presence of insulin in the liposomes.

3.5.2. Size determination and zeta potential

Zeta sizer analysis put on a better idea about the charge, size distribution, and polydisperse intensity (PDI) of the blank and insulin-loaded liposomes. In the values mentioned in Table 2, the average diameter of blank liposomes and insulin-loaded liposomes is 292.9 nm and 1294 nm, respectively. The zeta potential and PDI values of blank liposomes are –23.8 mV, and 0.404 respectively, and insulin-loaded liposomes bear −13.1 mV and PDI is 0.087 confirming the loading of insulin in liposomes. The charge on the particle decreases as the insulin is loaded onto it however upon loading the drug the size of the particle increases. The polydisperse intensity is the representation of the population of the particles in the given amount of the sample.

3.5.3. Stability analysis

Initially, the blank liposomes were translucent; however, insulin-loaded liposomes had a milky and runny appearance. Within 24 h, the viscosity and color of both liposomes; blank and insulin-loaded liposomes remained stable at 4°C. The color and viscosity of liposomes at 25°C had been changed steadily for two days, whereas the color and viscosity significantly remained unaltered at 4°C. Within 24 h, the liposomes began to attach at the bottom of a petri dish at 25°C and particle size decreased while at 4°C remain unaltered. The viscosity increased and the solution became cloudy after 48 h at 25°C. Moreover, Table 2 describes the zeta analysis of both blank and insulin loaded liposomes after 24 h, it can be seen that the size of insulin loaded liposomes changed to 1294 nm as compared to blank liposomes which had 292.9 nm, while the zeta potential changed from –23.8mv to −13.1mv. We suggest storing these liposomal nanocarriers in freeze dried form to retain their characteristic size and hypoglycemic potential.

3.5.4. Morphology of insulin-loaded liposomes by Scanning electron microscopy (SEM)

Scanning electron microscopic (SEM) graphics of the liposomes gave an idea about the clear morphology of the liposomes. It demonstrated a spherical shape in three dimensions that was uniformly smooth, encompassing a diverse spectrum of sizes ranging from substantial to minute, which were found to be in agreement with the characteristics of liposomes. However, the problem encountered here was that to go through the SEM the material has to be dried completely to sputter it with gold and fix it on the glass slides. If it fails to dry completely and any of the moisture remains in there, then the machine fails to give quality results. Hence the SEM of fresh samples was not possible. Fig. 7 showed the images of the samples under the SEM.

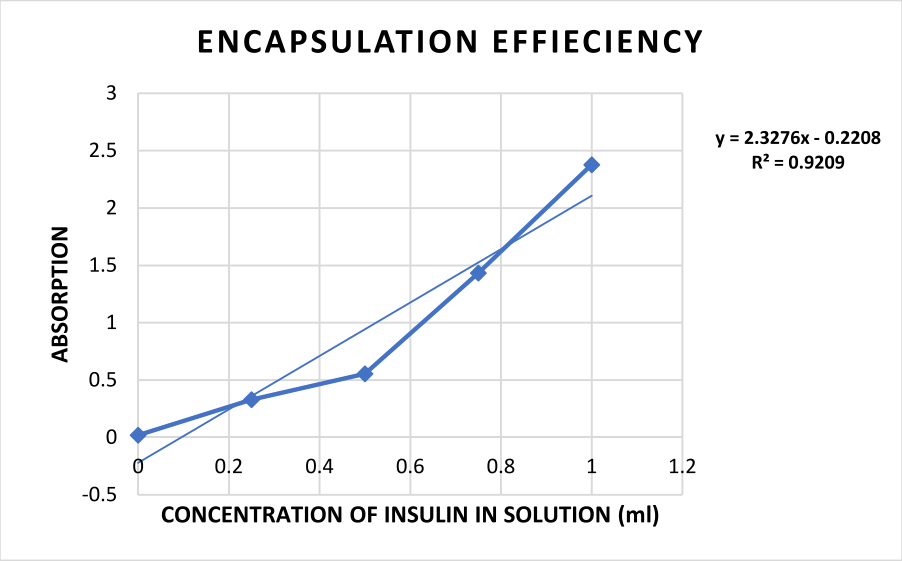

Fig. 2. A calibration curve of the encapsulation efficiency of insulin in liposomes at different concentrations. It was observed that the encapsulation efficiency of insulin in the liposomes was determined to be 34%.

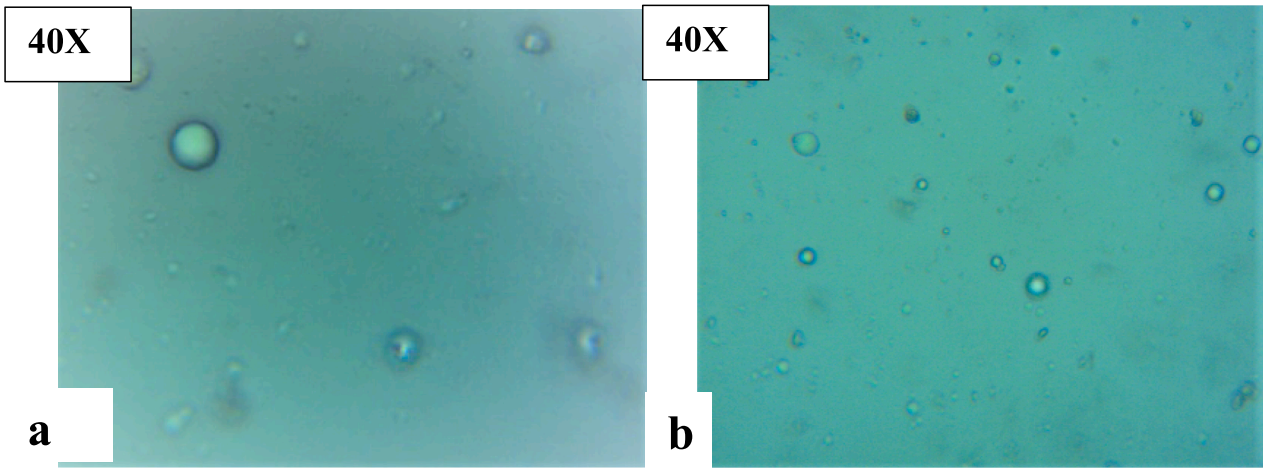

Fig. 3. Optical microscopic images of MFGM-based liposomes at 40X; (a) the morphology of Insulin loaded liposomes and (b) the morphology of Blank liposomes.

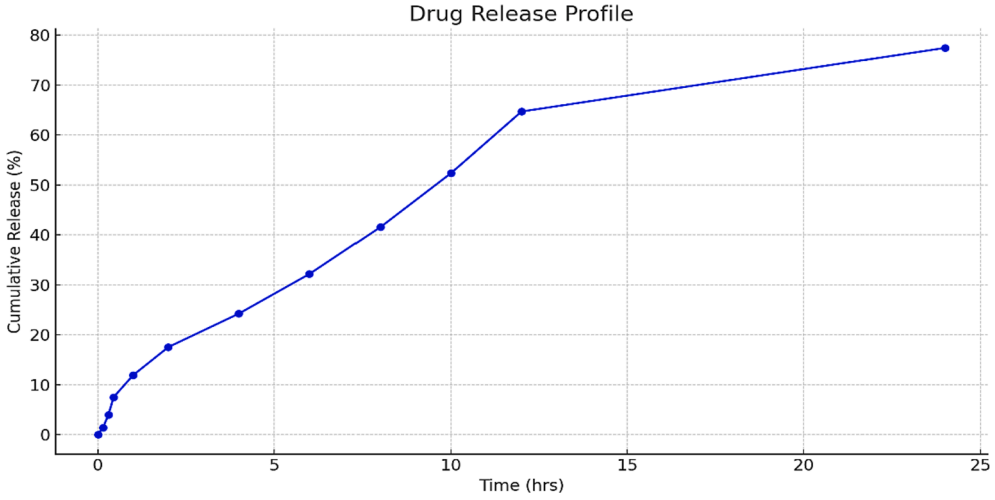

Fig. 4. *In vitro* release profiles of insulin from insulin loaded liposomes at pH 7.4.

Table 1
Kinetic model values for *in vitro* drug release.

Model	Parameter(s)	R^2
Zero Order	K0 = 4.0713	0.8784
First Order	K1 = 7.3312	0.8428
Higuchi	KH = 15.5838	0.9645
Korsmeyer-Peppas	K_KP = 12.0693, n = 0.6055	0.9722

3.6. *In vitro cytotoxicity and morphological analysis*

The MTT assay analysis is used to determine the safety profile of blank and insulin-loaded MFGM derived liposomes on normal HEK-293 cells. The assay revealed that cells treated with liposomes (both blank and insulin-loaded liposomes) showed high cellular viability. The cytotoxicity was closely related to that of control cells as the concentration of liposomes increased. The cell viability for both blank and insulin loaded liposome treated cells at 10%, 40 %, and 70 % is depicted in Fig. 8. The 10% showed the highest percentage of cell viability in both formulations; blank 94.2 %, insulin loaded liposomes 96.4%. Cellular morphology analysis revealed that cells were growing normally after they were treated with blank, and insulin-loaded liposomes. No change in morphology, behavior, or apoptosis was observed in treated cells after incubation for 24h with liposomes. This further verifies the finding that these liposomes are non-toxic to normal cells. Cell morphology pre- and post-treatment with blank and insulin-loaded liposomes is represented in Fig. 9.

3.7. *In vivo safety analysis*

3.7.1. *Hypoglycemic effect*

The blood glucose level of all the experiment groups for the 1st, 3rd, and 7th day is presented in Fig. 10. By applying One-way ANOVA, Sidak's multiple comparisons tests, a significant difference in post-treatment compared to their respective pre-treatment in the blood glucose level has been observed in all groups. The diabetic control group (DC) showed a significant increase in the blood glucose level compared to the control group (C) ($P < 0.0001$****). The significant adjusted *P*-value ($P < 0.0001$****) was observed by comparison with each group in pre- and post-treatment.

3.7.2. *Effect of insulin loaded MFGM derived liposomes on biochemical analysis*

1. Liver function test

The ALP, ALT, Bill, and Alb levels in all the experimental groups are represented in Fig. 11. The diabetic control group (DC) showed a significant increase in the ALP level compared to the control group (C) with adjusted value ($p = 0.0042$**) however, the treated group showed a significant decrease level of ALP enzyme in comparison to the DC. The results were obtained by applying One way ANOVA, Sidak's multiple comparisons tests, and adjusted p-value were observed. When the DC was compared with the DI and SCL it was observed ($p = 0.0035$**) and ($p = 0.0037$**) respectively. However, in the OL, the results were more significant by an adjusted p-value of 0.0011**. When the insulin-treated group compared with SCL and OL, there is non-significant results observed with adjusted p values (0.9311^{ns}) and (0.9655^{ns},) respectively. Moreover, the ALT level of DC was significantly increased in comparison to the C by an adjusted p-value (0.0146*). Whereas by comparing the ALT level were significantly decreased in the DI and SCL treated group by comparing to the DC the adjusted p-value was observed (0.0071**) and (0.0155*) respectively. For the OL, the ALT level in comparison to the DC was observed significantly improved level by an adjusted p-value of (0.0071**). When the DI compared with SCL and OL, there is non-significant results observed with adjusted p-value (0.7738^{ns}) and (0.9511^{ns}) respectively. Furthermore, the bilirubin level of the DC significantly increased when compared with the C with an adjusted p-value (0.0005***). However, for all the treatment groups the Bilirubin level significantly decreased as compared to the DC by adjusted p-value (<0.0001****). When the DI was compared with SCL and OL, there were nonsignificant results observed with adjusted p values (0.9894^{ns}) and (0.9894^{ns}) respectively.

The DC showed a non-significant increase in the Albumin level compared to the C ($p = 0.1731^{ns}$). The DI and SCL showed a significant decrease in the Albumin level by the adjusted p-value (0.0309*) and (0.0336*) respectively, however, the OL showed a significant decrease

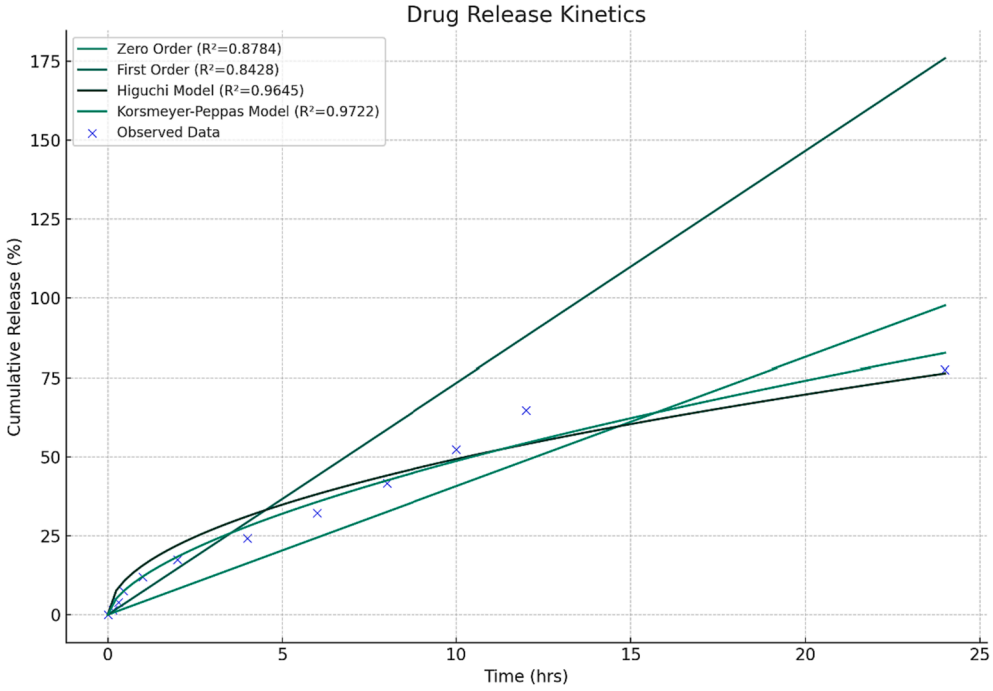

Fig. 5. Cumulative release profile of the drug delivery system over a 24-hour period, comparing observed data with various kinetic models including Zero Order, First Order, Higuchi, and Korsmeyer-Peppas.

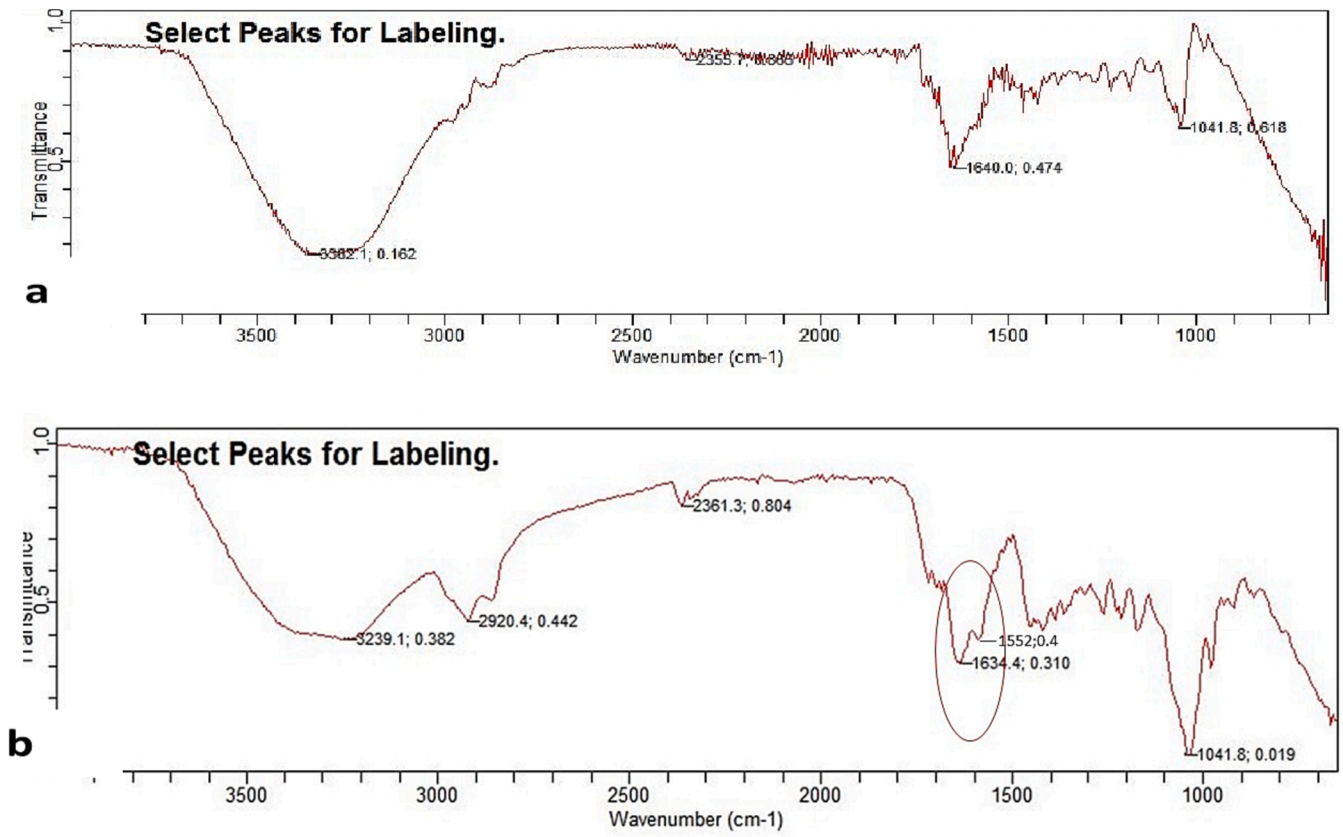

Fig. 6. FTIR spectra showed a peak on 1634 cm^{-1} and other peaks on 1552 cm^{-1}, both of these points are characteristic peaks of the protein spectra and can be referred to as amide-I and amide-II, respectively **(a)** FTIR spectrum of blank liposomes **(b)** insulin-loaded liposomes.

Table 2
Size and Zeta potential determination by zeta sizer.

Sr. No.	Type of Liposomes	Z-average (d. nm)	Zeta Potential (mV)	PDI
1	Blank Liposomes	292.9 nm	–23.8	0.404
2	Insulin Loaded Liposomes	1294 nm	−13.1	0.087

in the Albumin level by an adjusted p-value (0.0005***). When the DI compared with SCL and OL, there are non-significant results observed with adjusted p values (0.9565^{ns}) and (0.9565^{ns}) respectively.

ii. Renal functions test

The creatinine level of all the groups is represented in Fig. 12. The creatinine level of the diabetic group (DC) showed a non-significant increase compared to the control group (C) ($p = 0.1181^{ns}$). Whereas all the other groups showed a decreasing trend in comparison to the diabetic group with adjusted ($p < 0.0001$****). Though when the insulin-treated group (DI) compared with subcutaneous-treated liposomes (SCL) and orally treated liposomes (OL), there is non-significant results observed with adjusted *p*-value (0.8360^{ns}) and (0.5980^{ns}) respectively. Likewise, the non-significant decrease in uric acid level with adjusted *p*-value (0.1017^{ns}) for the diabetic rats (DC) has been observed in comparison to the control group (C). In all the treatment

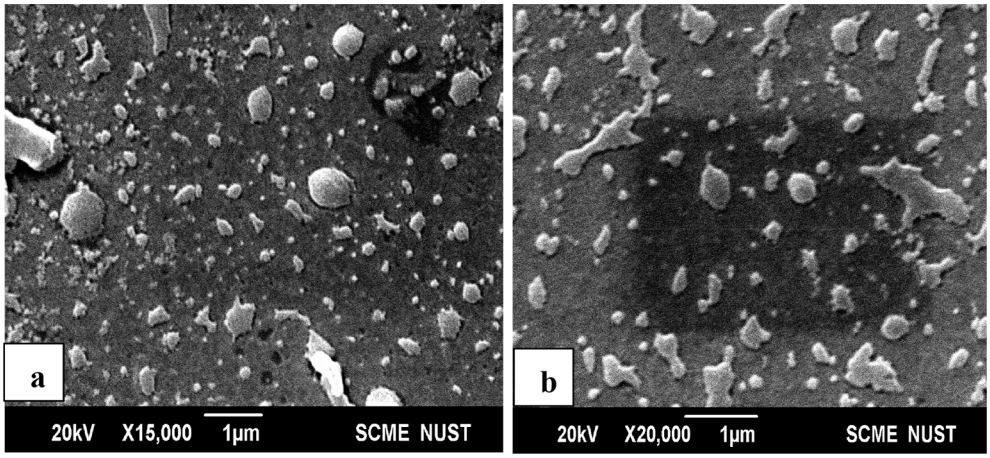

Fig. 7. SEM images of MFGM-derived liposomes showed a smooth 3D sphere shape with different sizes, similar to liposomes. **(a)** at 15,000X and **(b)** 20,000X at 1um area.

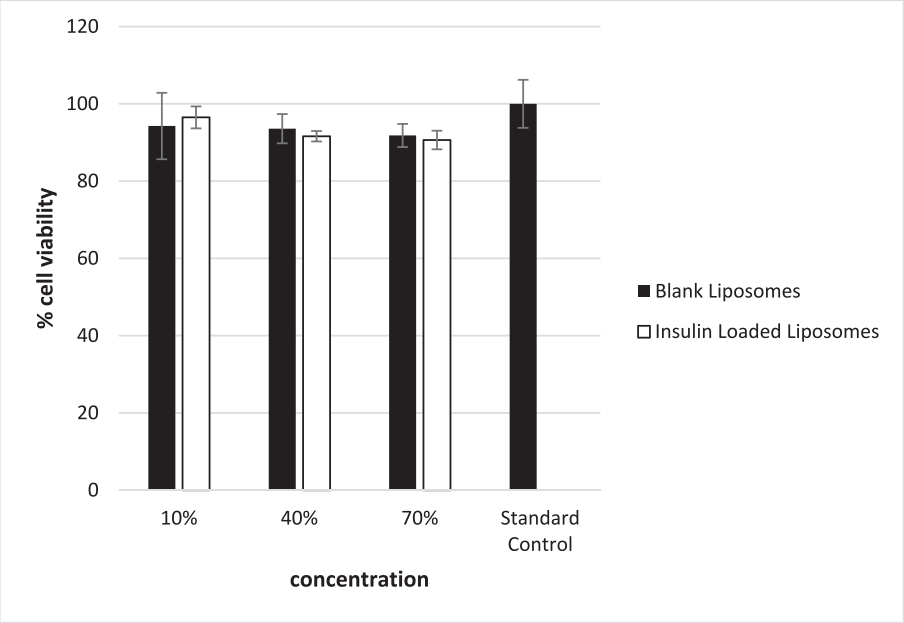

Fig. 8. Percentage cell viability analysis via MTT assay of both insulin-loaded and blank liposomes.

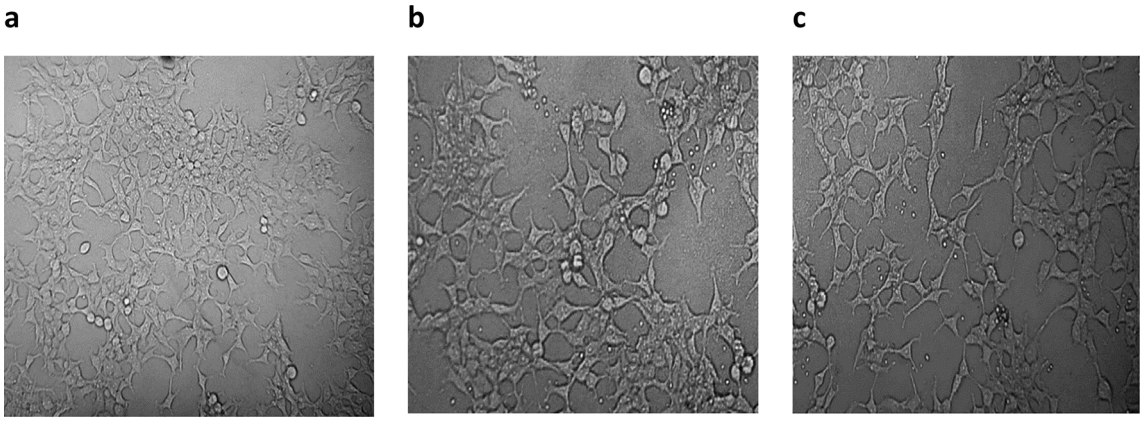

Fig. 9. Cell morphology analysis: **(a)** HEK-293 cells before treatment with liposomes **(b)** HEK-293 cells 24 h post-treatment with blank liposomes **(c)** HEK-293 cells 24 h post-treatment with insulin-loaded liposomes.

groups nonsignificant results were observed in comparison to the diabetic group (DC) and insulin-treated groups (DI).

3.8. Histopathological analysis

3.8.1. histology of liver tissue

To determine the treatment effect of the MFGM-derived insulin-loaded liposomes on the liver tissues of STZ-induced diabetic rats, simple light microscopy was used to visualize and analyze the histopathological slides at 40X. It can be seen in Fig. 13, that group 1, which is a control group (C), were not given any treatment, hence in the tissue analysis normal structure and cellular physiology were observed. The hepatic artery, portal vein, and interlobular duct which is known as the portal triad runs clearly around the periphery of each lobule and configure hexagonal kind plate formation. Sinusoids, the small thin veins that divide the hexagonal plates and darkly stained Kupffer cells can be viewed. In liver tissue-stained micrographs of group 2 which is the diseased diabetic (DC) group and did not undergo any treatment, inflammation can be observed. Severe hepatocyte death, congestion of the central vein, along with loss of hepatic lobule, nuclear condensation, loss of sinusoidal space, fibrosis, and penetration of leukocytes near the central vein was also observed. Dark stained irregular hepatocytes and damaged nuclei here represent the necrosis. While Group 3 (DI), was treated with insulin subcutaneously, the micrographs of the liver tissue of this group also showed the congestion of the central vein and destructive changes. However, some recovered areas can also be observed. Normal liver histology of group 4 (SCL) and group 5 (OL) were observed, however, some signs of liver apoptosis and loss of sinusoidal space were also observed in SCL treated group.

3.8.2. Histology of renal tissue

Renal histopathology of the Control group (C) indicated a well-organized cellular structure in the visualized section Fig. 14. Histological section (a) of the cortical region showed normal glomerulus and intact bowman's capsule and proximal tubule having brush border membrane. No signs of glomerulopathy or tubulitis could be seen. The medullary region shows a normal striped appearance of collecting ducts, no signs of inflammation can be observed in the section under observation. Group 2 (b) which is a diseased group (DC) shows loss of normal glomerulus texture and loss of bowman capsule can also be observed, leukocytosis can be observed in both cortical and medullary regions. Loss of normal striped appearance in the medullary region can also be

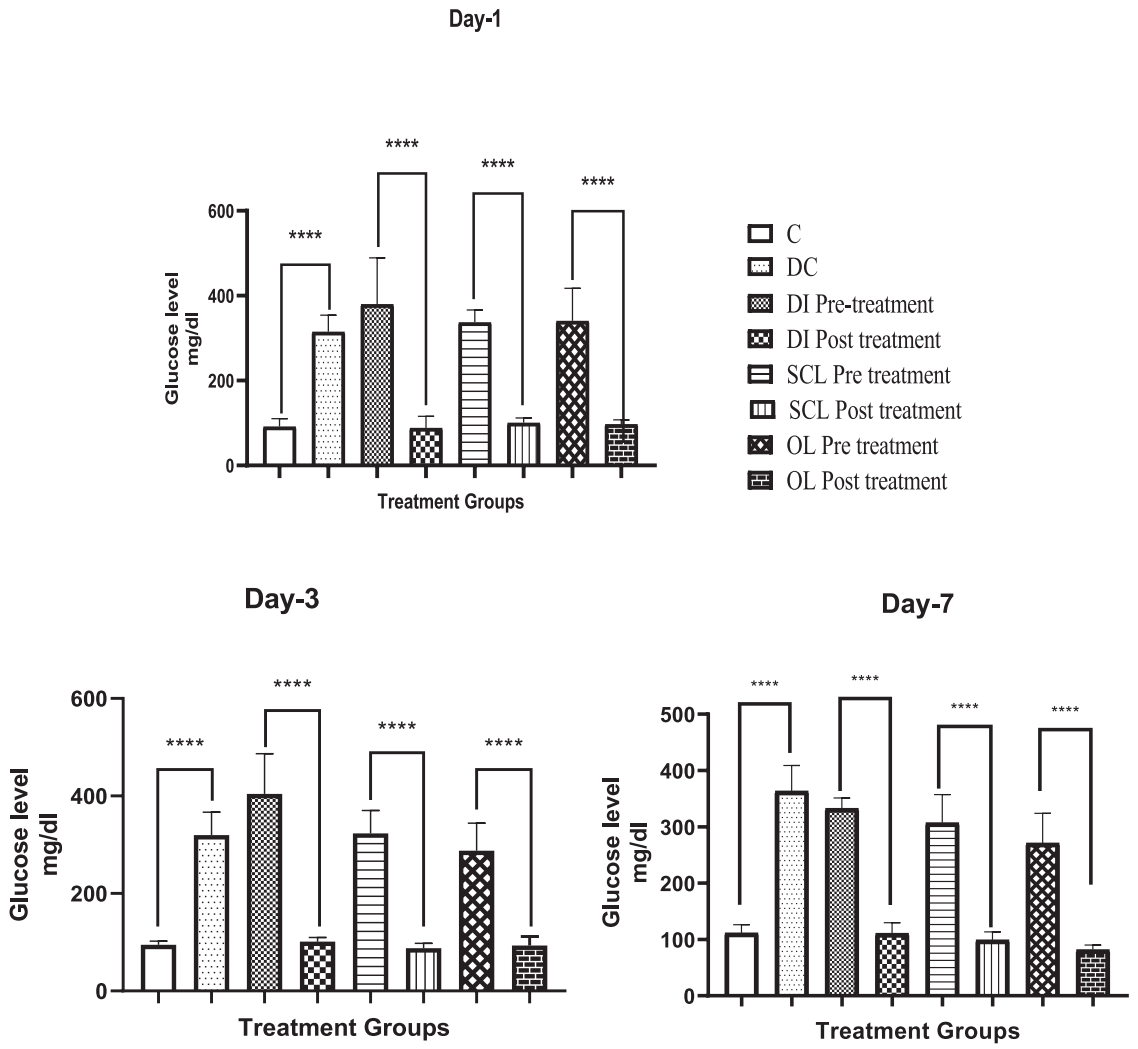

Fig. 10. Pre and post-treatment of insulin-loaded liposomes: The results showed a significant decrease in glucose levels after post-treatment than pre-treatment of all the treatment groups by day 1, 3, and day 7 with ($P < 0.0001$****).

observed in the section under visualization. However, the cellular structure appears normal and much similar to the control group in the rest of all the other groups i.e., (c) in group 3, (d), in group 4, and (e) in group 5, which are different treatment groups. Recovery of the cortex and medulla can be seen with few foci of inflammation in both regions can be observed in visualized sections.

4. Discussion

In developing nations, diabetes mellitus is becoming a prevalent chronic ailment, particularly noteworthy due to the gravity of its complications. This disease has been identified as a public health concern due to an array of factors including population expansion and aging, augmented urbanization, escalating rates of obesity and sedentary lifestyles, and the amplified survival rate of individuals affected with diabetes. Diabetes is the most prevalent chronic metabolic illness in the world and one of the top five leading causes of death. It is rapidly spreading across the globe, with an estimated 300 million individuals impacted by 2025. Diabetes is defined by an innate or acquired inability to secrete insulin, which results in an increase in blood glucose levels, which has a detrimental effect on various physiological systems. Hyperglycemia is the most prevalent clinical manifestation of diabetes, which is associated with the onset of certain problems, including the formation of oxygen radicals (ROS) in the body and pancreatic injury, and may be responsible for elevated blood glucose levels in animals. STZ results in hyperglycemia by disrupting the beta cells in the pancreas, which produce insulin from cells endocrine (Płaczek et al., 2019). At an advanced stage of diabetes onset, patients are unable to produce insulin from the pancreas due to cellular failure, and hence exogenous insulin is administered to simulate the physiological production of insulin in the body in an attempt to maintain glycemic control (Aqib et al., 2019). Insulin aids in the maintenance of glucose from the bloodstream and into cells. Your cells use a portion of the sugar for energy and then store the remainder in fat, muscles, and liver.

In comparison to alternative systemic routes of administration, administering insulin via the oral route has various advantages. For example, eliminate the local pain, discomfort, irritation, needlestick damage, and danger of skin infection caused by *Staphylococcus aureus* and *Mycobacterium chelonae*. In normal human metabolism, the pancreas detects an increase in blood glucose following a meal and secretes insulin to maintain an appropriate glucose level. Thus, the primary advantage of oral insulin is that it may be least painful to administer than a conventional injection of insulin, where the injection site could become hypersensitive and irritated with time (Aqib et al., 2019).

MFGM is derived from the mammary gland epithelium and is a complicated mixture of 40 percent lipids and almost 60% protein. Phospholipids are the major constituent of the MFGM and are required for the formation of liposomes. Glycerophospholipids which are

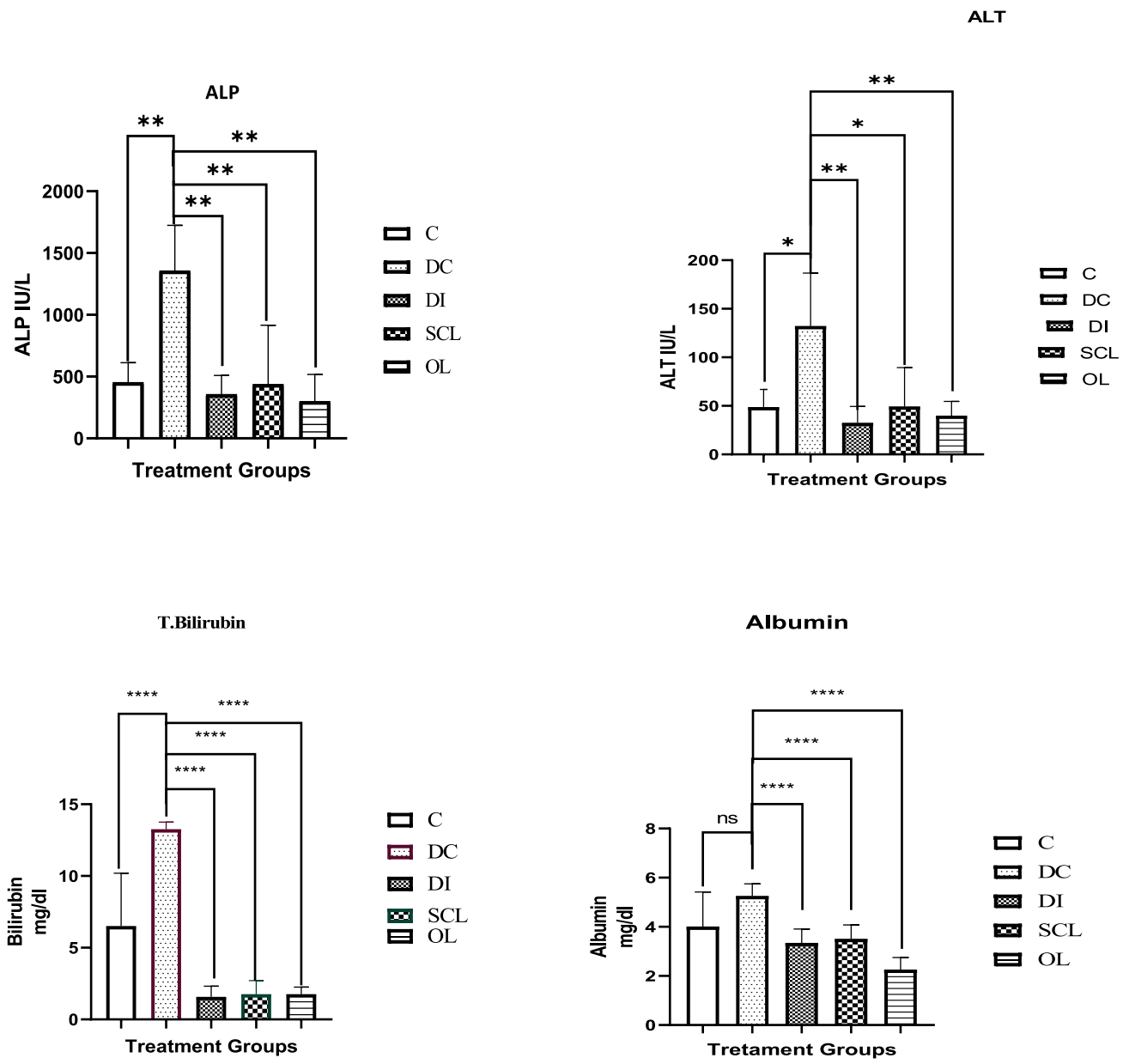

Fig. 11. Variations in liver enzymes; the results showed a significant decrease in the ALP, ALT, bilirubin, and albumin level of all treatment groups. The overall significant results were observed summarized *p*-value is (0.0016**), (0.0068**), (<0.0001****) and (0.0022**), respectively.

membrane-based phospholipids are a major portion of these phospholipid and contain, phosphatidylethanolamine (PE), phosphatidylcholine (PC), Sphingolipids that majorly includes the Sphingomyelin (SM), phosphatidylinositol (PI) and phosphatidylserine. PE, PC, and SM make up the major portion (Rebolledo-Solleiro and Fernández-Guasti, 2018). Liposomes can be made using phospholipids generated from MFGM. The high sphingolipid content of MFGM phospholipids may confer nutritional benefits on the user while also enhancing liposome activity. The goal of this research was to make the liposomes loaded with insulin from camel milk derived MFGM as an oral insulin solution. The MFGM was extracted and liposomes were formed by thin film hydration (Niu et al., 2012).

The amide I region of proteins between 1600 cm^{-1} and 1700 cm^{-1} is mostly constituted of various bands related to secondary structural features such as α-helices, β-sheets, twists, and arbitrary conformations. The backbone shape and hydrogen bonding arrangement dictate the exact band position. The protein-specific amide II spectra insulin monomer has several ionizable cationic or anionic groups as a result of six amino acid residues that can acquire a positive charge and ten amino acid residues that can acquire a negative charge. It is much more complex than amide I and is found between 1510 cm^{-1} and 1580 cm^{-1}. As an interception of values obtained in FTIR, it predicted that insulin encapsulated in liposomes (Refai and Hassan, 2017). Zeta potential of +10 mV to −10 mV is generally considered neutral and if zeta potential is of +30 mV or greater than or −30 mV or lesser than it then the particles tend to behave stable (Singh et al., 2019). In our study, the zeta potential of both loaded and blank liposomes is within this range of stability; nevertheless, the charge of the insulin-loaded particles decreases following loading due to the presence of a positive charge on insulin. The acceptable value of the polydispersity index always is less than 0.7 which happens in the case of both blank and insulin-loaded liposomes which is a sign of good homogeneity (Swelum et al., 2021). The particle size increases upon loading the drug and varies differently according to the solution, in our solvent the loaded liposomes showed an average size of 1294 nm with 0.087 PDI and blank liposomes had an average size of 292.9 nm with a PDI value of 0.404. The increase in the

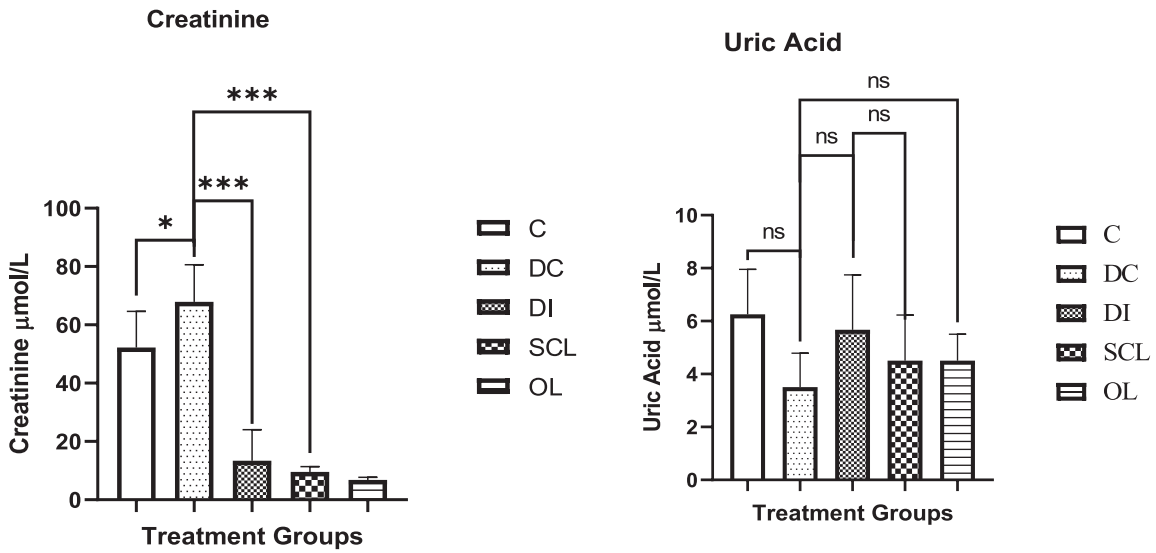

Fig. 12. The changes in renal parameters showed a non-significant increase in the creatinine level of the diabetic group (DC) compared to the control (C), whereas the overall significant decrease in the creatinine level of all treatment groups with the ($p<0.0001$****) has been observed. However, a decreasing trend has been observed with the summarized p value (=0.1770 ^{ns}).

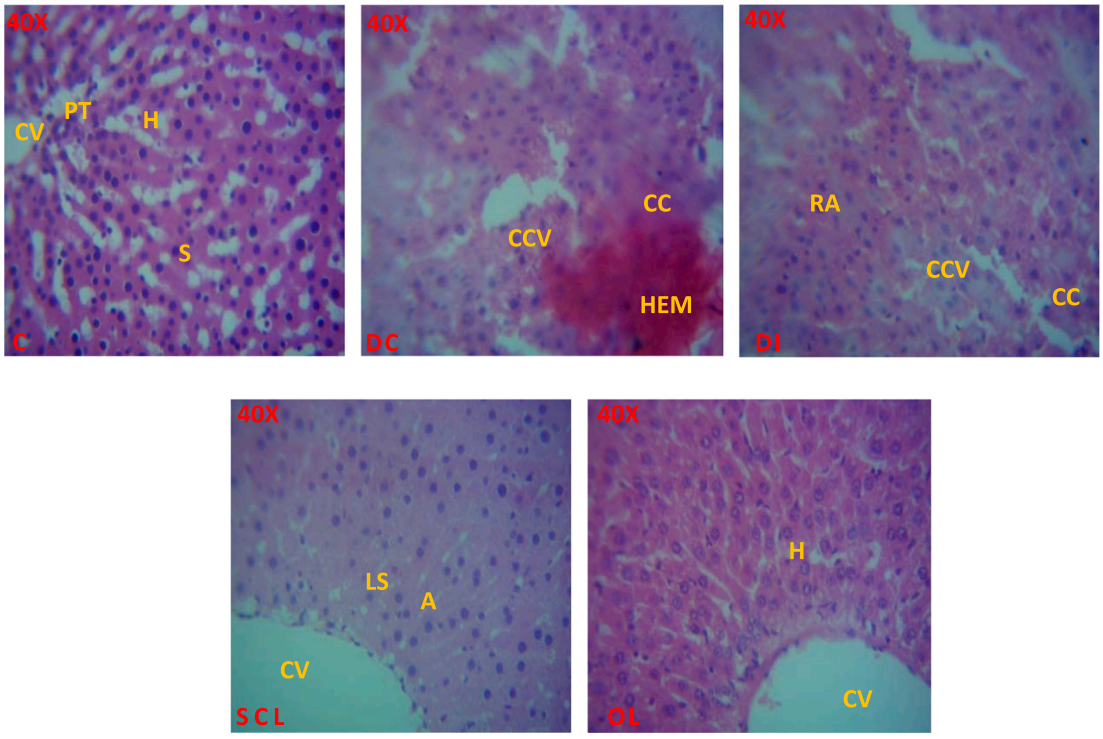

Fig. 13. Micrographs of liver histology (40X): Micrographs of the disease group (DC) represent the loss of normal hepatic parenchymal architecture with swelling of hepatocytes, cellular clumping (CC), and Loss of sinusoidal space. Foci of hemorrhage (Hem) can also be observed. The Insulin treated (DI) samples show recovery from inflammation hepatocytes arranging themselves near the central vein with the restoration of normal sinusoidal space and recovered patches. The subcutaneously treated group (SCL) showed hepatocytes arranging themselves near the central vein, which also represents the loss of restoration of sinusoidal space. While the group with orally treated liposomes (OL) showed normal liver histology, hepatocytes cordially arrange near the central vein and normal structure of hepatocytes. Central Vein (CV), Portal triad (PT), Sinusoidal space (S), Hepatocytes (H), cell clumping (CC).

size of the particle after loading insulin has been previously reported in the literature (Thompson and Singh, 2006). The size of the loaded drug can be drilled down according to the requirement by using the extrusion filtration process. SEM analysis revealed a smooth three-dimensional sphere shape with a range of sizes from large to small size compatible with liposomes, these results are compliant with conventional MFGM-based liposome results (van der Veen et al., 2017). Both the encapsulation efficiency and size of the liposomes depend upon the hydration media. The encapsulation efficiency of our formulation is 34 percent, the hydration media used in this research was PBS which in general tends to lower the encapsulation efficiency of the particle (Thompson and Singh, 2006).

The current investigation examines the distinctive attributes of liposomes made from lipid bilayers obtained from the membrane

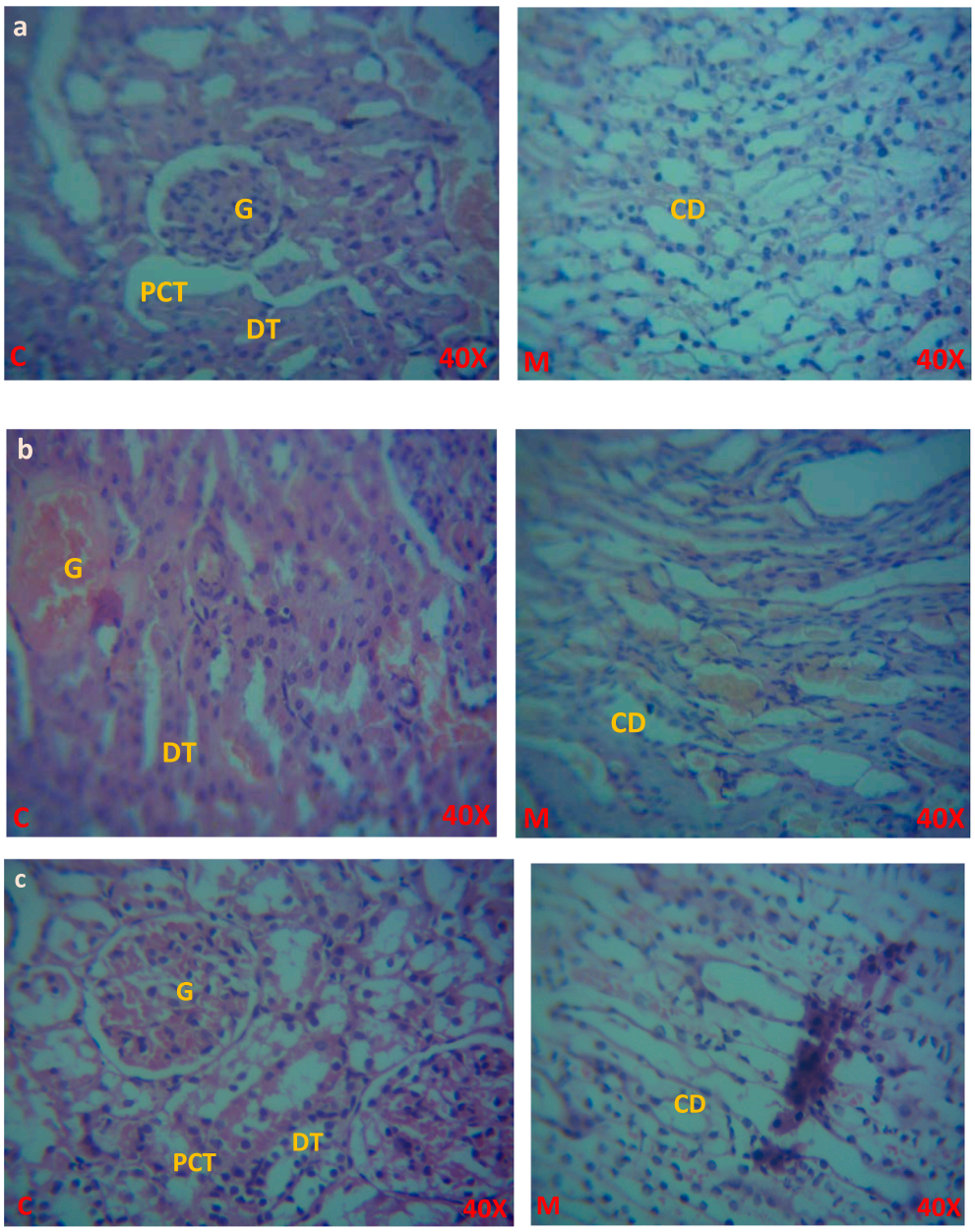

Fig. 14. Micrographs of Renal histology (40X): (a) Control group, cortical region (C) shows normal glomerulus (G) and intact bowman's capsule and proximal tubule (PCT) having brush border membrane. Normal stripped appearance in medullary (M) region. (b) Disease group, Loss of normal glomerulus texture can be observed with loss of bowman capsule, leukocytosis can also be observed in both regions, and Normal striped appearance loss in the medullary section. (c) Insulin treated group, (d) Subcutaneous liposomes treated group, (e) Orally treated liposomes group, visualize sections all these groups show the recovery of cortex and medulla with few foci of inflammation in both regions.

surrounding fat globules in camel milk, known as the milk fat globule membrane (MFGM). The study also investigates how these liposomes can be used to encapsulate and release insulin. The precise composition and structure of these liposomes, derived from camel MFGM, have a crucial impact in determining the insulin release profile. The lipid content and surface charge of liposomes produced from camel MFGM may differ greatly from those of conventional liposomes, indicating a potentially different interaction with insulin. This interaction is intriguing since the camel MFGM is believed to offer protection to insulin-like peptides found in camel milk, this property could result in a non-Fickian diffusion release profile. The divergence from conventional diffusion models suggests an intricate interaction within the liposome and the encapsulated insulin (Van Hoogevest, 2014).

Additionally, the relationship between insulin, a protein, and the liposomal membrane is another crucial determinant affecting the release process. The diverse levels of attraction that insulin exhibits towards the lipid layers of the liposome can lead to a release pattern that deviates from the principles of straightforward diffusion. This aspect emphasizes the intricacy of the drug release mechanism from these liposomes and emphasizes the need for a detailed understanding of the insulin-liposome interaction.

In current research, the cytotoxic effect of MFGM-derived liposomes on the HEK-293 cell lines is the non-tumor epithelial cells were chosen to observe the effect of insulin-loaded and blank liposomes on the origin, morphology, and viability of cells (Wong and Al-Salami, 2017). All the exposed solution showed a cell viability value more than 90 percent

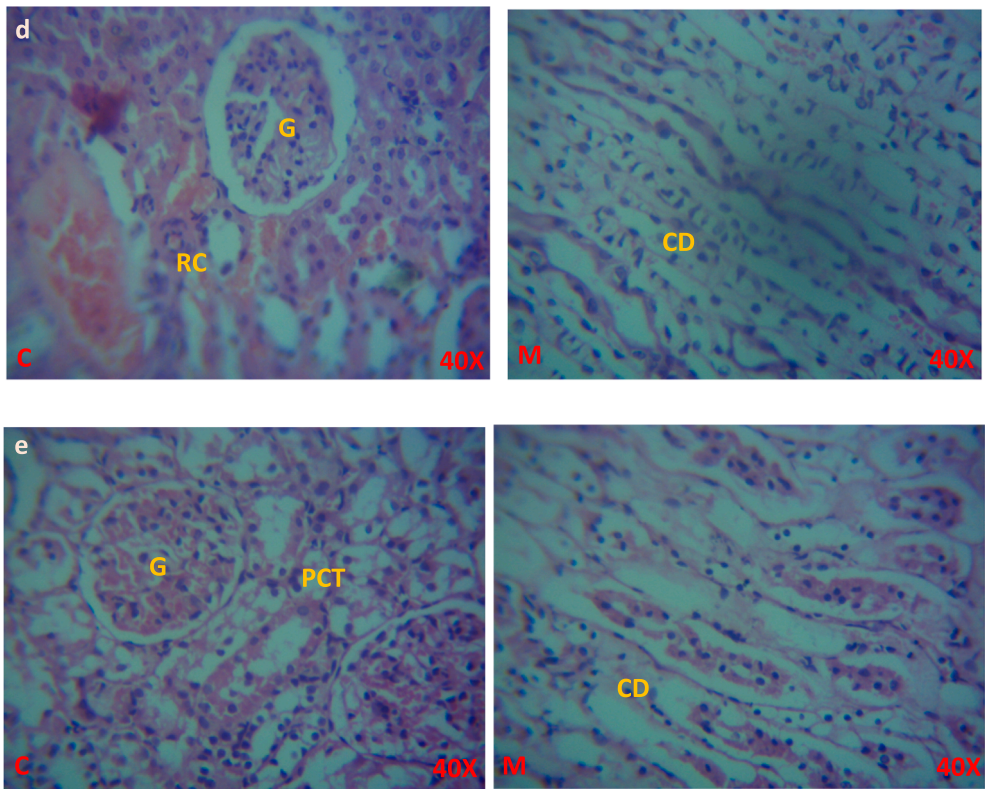

Fig. 14. (*continued*).

which means that liposomes used in this study has no significant cytotoxic effects, these results are in compliance with the already published study (Thompson and Singh, 2006).

All experimental groups showed a significant hypoglycemic effect in STZ-induced diabetic rats after 4 h of the treatment. The increase in blood insulin level is in direct correlation with the decrease in blood glucose level, and this correlation of results indicates the fact of efficacy and absorption of liposomes via the oral route (Aboonabi et al., 2014).

In diabetic rats, a substantial rise in common enzymatic biomarkers (ALP, ALT, Bilirubin,) of Liver functioning was reported. Numerous factors can contribute to abnormal liver function tests in diabetes patients. To begin, hyperinsulinemia may result in hepatic insulin resistance and lipid abnormalities. It is well known that growing hepatic fat accumulation is harmful to hepatocytes, raising transaminases and decreasing the liver's ability to synthesize new cells (Wong and Al-Salami, 2018). A higher quantity of albumin is linked to kidney and liver disease, as well as a quicker rate of water loss from the body. A rise in serum albumin implies decreased liver production or function, which may be brought on by harmed liver cells or a reduction in protein intake (Wong and Al-Salami, 2018). The presence of numerous dark-stained shrunken hepatocytes and tiny dark nuclei demonstrated the loss of normal hepatic architecture in the diseased group however the recovery in the liver damage of the orally treated group (OL) has been observed also the signs of restoration of the lost sinusoidal space has also been observed in the subcutaneously injected liposomes treatment group. PC/PE ratios that are abnormally high or low affect energy metabolism and are associated with liver disease progression. Phospholipids are also majorly known for their antioxidant, anti-inflammatory, and apoptosis-modulating responses, whereas the liposomes prepared from the MFGM which contains a wide variety of phospholipids have also potentially played a role in the recovery of biomarkers in the normal range which is also a sign of liver damage recovery (Wong and Martinez, 2016). While kidney functions (creatinine and uric acid) were found to be non-significant in treated experimental groups. Serum creatinine and uric acid levels are used as indicators of nephrotoxicity in the diagnosis of kidney injury. In a histopathological analysis of the kidney, the disease group (DC) showed the atrophy of the glomerulus and deformation of the renal corpuscle along with the loss of the normal striped appearance of the medullary region. The treatment group showed a resistance to kidney damage and the cellular structure tissue histopathology of all treatment groups appeared to be intact and normal. This could be because of the sort of rats employed in the study or the experiment's short duration (Wong and Al-Salami, 2018). In a histopathological analysis of the kidney, the disease group (DC) showed the atrophy of the glomerulus and deformation of the renal corpuscle along with the loss of the normal striped appearance of the medullary region. The treatment group showed resistance to kidney damage and the cellular structure tissue histopathology of all treatment groups appeared to be intact and normal (Yücel et al., 2019).

This study demonstrates that oral administration of insulin-loaded liposomes derived from camel milk fat globule membrane (MFGM) effectively induces hypoglycemic effects in STZ-induced diabetic rats and can be used as promising carrier for oral insulin delivery. The study's foundation was based on the hypothesis that the MFGM is a unique phospholipids and sphingolipids possess antidiabetic properties and could enhance the oral bioavailability of insulin (Jabs AJJLoBM, 2005). By extracting MFGM from camel milk and preparing laboratory liposomes loaded with insulin, the research provided evidence supporting this hypothesis, showing a significant reduction in hyperglycemia. Future research endeavors will focus on expanding the scope of this study to larger animal models and experimenting with various liposomal formulations. A critical aspect of upcoming studies will include conducting in-depth immunogenicity analyses to ensure the safety and efficacy of these liposomal formulations. This next phase is expected to yield further insights into the potential of MFGM-derived liposomes as an innovative oral insulin delivery system, paving the way for novel therapeutic approaches in diabetes management. The study also emphasizes the need for deeper understanding of the interactions between

insulin and liposomal membranes, which influence the drug release mechanism.

5. Conclusion

Insulin is considered the primary therapy for the diabetic cure. However, owing to the proteolytic digestion in the stomach it needs to be administered subcutaneously into the body which does not fall in patient compliance. Camel milk has been used for a long time by nomadic people because of its natural anti-diabetic potential. Came milk possess certain phospholipids that aids the hypoglycemic and anti-hypertensive activity, MFGM contains the major chunk of phospholipids, these camel milk derived MFGM, however, has never been used in the formation of liposomes for encapsulating insulin for oral delivery. In this study, camel milk-derived MFGM was used to make liposomes which were then loaded with insulin and evaluated *in vitro* and *in vivo* on STZ-induced diabetic rats. Zeta, along with FTIR and SEM methods, were employed to characterize both blank and insulin-loaded liposomes. These liposomes were then administered via mucosal and subcutaneous routes in a series of *in vivo* experiments. In *in vitro* analysis, these liposomes showed more than 90 percent cell viability at all concentrations (70 %, 30 %, and 10 %). *In vivo* analysis of both the orally treated and subcutaneously treated liposomal group showed a significant hypoglycemic effect compared to the diabetic group. The given treatment also improved the normal liver functioning biomarkers. Significant changes were observed in the histopathological analysis of the liver and no significant changes were observed in the kidney. The study concludes successfully that Camel MFGM insulin loaded liposomes when given orally provides the hypoglycemic effects in the STZ induced diabetic rats. Additional extended-duration experiments are necessary to ascertain the longevity of the hypoglycemic effect. Enhancing the insulin loading capacity of the liposomes through coating techniques, combining them with other drugs for prolonged activity, and conducting shelf-life studies are also crucial steps for further research.

Funding

This research work was funded by Institutional Fund Projects under grant no. (IFPIP: 396-290-1443). The authors gratefully acknowledge the technical and financial support provided by the Ministry of Education and King Abdulaziz University, DSR, Jeddah, Saudi Arabia".

Declaration of competing interest

The authors declare that they have no known competing financial interests or personal relationships that could have appeared to influence the work reported in this paper.

Acknowledgment

The authors would like to thank the animal house faculty of the Atta-Ur-Rahman School of Applied Biosciences (ASAB), National University of Sciences and Technology (NUST), Islamabad, Pakistan for their help and guidelines in conducting the *in-vivo* experimental work. We would also thank Dr. Ramish Riaz Assistant Professor (Head of Department, Medical Imaging Technology) at Riphah International University, for her help in conducting the statistical analysis and histopathological study of this work.

Disclosure statements

This research work was funded by Institutional Fund Projects under grant no. (IFPIP: 396-290-1443). The authors gratefully acknowledge the technical and financial support provided by the Ministry of Education and King Abdulaziz University, DSR, Jeddah, Saudi Arabia".

Authors contribution

The project design and concept layout by SS and TA; SS and FI were directly involved in the experimental work and writing the manuscript. KK conducted the *In-vitro* experiments; TA supervised this project. Data analysis, methodology, and funding by MSA, SA provided technical support and proofread this article. All authors contributed equally to conducting the experiment, writing, reviewing, or editing the manuscript before submission.

Ethical consideration

Animal ethics

The animals were obtained from the Animal House facility of Atta-Ur-Rahman School of Applied Biosciences (ASAB) of the National University of Sciences and Technology (NUST), Islamabad, Pakistan. All animal procedures and studies were undertaken with the agreement of the Institutional Review Board (IRB) Ref. IRB No. 11-2020-01/03 and all experimental standard protocols followed and approved by the Laboratory animal house (LAH), ASAB, and NUST.

References

Aboonabi, A., Rahmat, A., Othman, F.J.J.C.H., 2014. Effect of pomegranate on histopathology of liver and kidney on generated oxidative stress diabetic induced rats. 2014;6(1):2-5.

Abud, M.B., Louzada, R.N., Isaac, D.L.C., Souza, L.G., Dos Reis, R.G., Lima, E.M., et al., 2019. In vivo and in vitro toxicity evaluation of liposome-encapsulated sirolimus 2019;5(1):1–10.

Ali, A,H., Zou, X., Abed, S.M., Korma, S.A., Jin, Q., Wang, X.J.Crifs., et al. Natural phospholipids: occurrence, biosynthesis, separation, identification, and beneficial health aspects. 2019;59(2):253-75.

Anwar, I., Khan, F.B., Maqsood, S., Ayoub, M.A.JFiN, 2021. Camel milk targeting insulin receptor—toward understanding the antidiabetic effects of camel milk. 2021;8.

Aqib, A.I., Kulyar, M.F.-e.-A., Ashfaq, K., Bhutta, Z.A., Shoaib, M., Ahmed, R.J.T.i.F.S., et al. Camel milk insuline: Pathophysiological and molecular repository. 2019;88: 497-504.

Arranz, E., Corredig, M.J.J.o.d.s., 2017. Invited review: Milk phospholipid vesicles, their colloidal properties, and potential as delivery vehicles for bioactive molecules. 2017; 100(6):4213-22.

Ayoub, M.A., Palakkott, A.R., Ashraf, A., Iratni, R.J.D.R., Practice, C., 2018. The molecular basis of the anti-diabetic properties of camel milk. 2018;146:305-12.

Bakry, I.A., Yang, L., Farag, M.A., Korma, S.A., Khalifa, I., Cacciotti, I., et al., 2021. A comprehensive review of the composition, nutritional value, and functional properties of camel milk fat. 2021;10(9):2158.

Balamash, K.S., Alkreathy, H.M., Al Gahdali, E.H., Khoja, S.O., Ahmad, A.J.J.o.D.R., 2018. Comparative biochemical and histopathological studies on the efficacy of metformin and virgin olive oil against streptozotocin-induced diabetes in Sprague-Dawley rats. 2018;2018.

Chai, C., Oh, S., Imm, J.-Y.J.F.S.o.A.R., 2022. Roles of milk fat globule membrane on fat digestion and infant nutrition. 2022;42(3):351.

Clogston, J.D., Patri, A.K., 2011. Zeta potential measurement. Springer, Characterization of nanoparticles intended for drug delivery, pp. 63–70.

Contarini, G., Povolo, M.J.I.J.o.M.S., 2013. Phospholipids in milk fat: composition, biological and technological significance, and analytical strategies. 2013;14(2): 2808-31.

Evers, J.M., Haverkamp, R.G., Holroyd, S.E., Jameson, G.B., Mackenzie, D.D., McCarthy, O.J.J.I.D.J., 2008. Heterogeneity of milk fat globule membrane structure and composition as observed using fluorescence microscopy techniques. 2008;18(12): 1081-9.

Hameed, A., Ishtiaq, F., Zeeshan, M., Akhtar, S., Ismail, T., Ahmad, R.S., et al., 2023. Combined antidiabetic potential of camel milk yogurt with Cinnamomum verum and Stevia rebaudiana by using rodent modelling. 2023;60(3):1175-84.

He, H., Lu, Y., Qi, J., Zhao, W., Dong, X., Wu, W.J.A.P.S.B., 2018. Biomimetic thiamine-and niacin-decorated liposomes for enhanced oral delivery of insulin. 2018;8(1): 97–105.

Ibišević, M., Smajlović, A., Arsić, IJTASpjoc, technology, 2019. Optimization of high pressure homogenization in the production of liposomal dispersions 12(2), 7–10.

Ismail, T., Ahmad, Z., Sestili, P., Hussain, M., Akram, K., Ismail, A., et al., Camel's milk concentrate inhibits streptozotocin induced diabetes. 2018;26:73-9.

Izadi, A., Khedmat, L., Mojtahedi, S.Y.J.J.o.F.F., 2019. Nutritional and therapeutic perspectives of camel milk and its protein hydrolysates: a review on versatile biofunctional properties. 60, 103441.

Jabs, A.J.J.L.o.B.M., 2005. Determination of secondary structure in proteins by fourier transform infrared spectroscopy (FTIR), 2005.

Jash, A., Ubeyitogullari, A., Rizvi, S.S.J.G.C., 2020. Synthesis of multivitamin-loaded heat stable liposomes from milk fat globule membrane phospholipids by using a supercritical-CO 2 based system 22(16), 5345–56.

Jash, A., Rizvi, S.S.J.I.F.S., Technologies E., 2022. Heat-stable liposomes from milk fat globule membrane phospholipids for pH-triggered delivery of hydrophilic and lipophilic bioactives 79, 103030.
Lee, H., Padhi, E., Hasegawa, Y., Larke, J., Parenti, M., Wang, A., et al., Compositional dynamics of the milk fat globule and its role in infant development. 2018;6:313.
Liu, W., Ye, A., Liu, W., Liu, C., Singh, H.J.J.o.D.S., 2013. Stability during in vitro digestion of lactoferrin-loaded liposomes prepared from milk fat globule membrane-derived phospholipids 96(4):2061–70.
Liu, Y., Zhou, C., Song, Z., Li, L., Wang, H., Xia, X., et al., 2020. Insulin-lipid complex, preparation method therefor, and preparation thereof. Google Patents.
Malik, A., Al-Senaidy, A., Skrzypczak-Jankun, E., Jankun, J.J.I.j.o.m.m., 2012. A study of the anti-diabetic agents of camel milk 30(3), 585-92.
Malik, P., Danthine, S., Paul, A., Blecker, C.J.S.B.S.F., 2015. Biotechnologies. Physical-chemical properties of milk fat globule membrane at different stages of isolation. 2015;19:154–9.
Maswadeh, H.M., Aljarbou, A.N., Alorainy, M.S., Alsharidah, M.S., Khan, M.A.J.B.R.I., 2015. Etoposide incorporated into camel milk phospholipids liposomes shows increased activity against fibrosarcoma in a mouse model. 2015.
Matteucci, E., Giampietro, O., Covolan, V., Giustarini, D., Fanti, P., Rossi, R.J.D.D., Development, et al., 2015. Insulin administration: present strategies and future directions for a noninvasive (possibly more physiological) delivery. 2015;9:3109.
Mirmiran, P., Ejtahed, H.-S., Angoorani, P., Eslami, F., Azizi, F.J.I.j.o.e., metabolism, 2017. Camel milk has beneficial effects on diabetes mellitus: a systematic review. 2017;15(2).
Nagarchi, K., Ahmed, S., Sabus, A., Saheb, S.H.J.J.o.P.S., 2015. Research. Effect of streptozotocin on glucose levels in albino Wister rats. 2015;7(2):67.
Nguyen, T.X., Huang, .L, Liu, .L, Abdalla, A.M.E, Gauthier, M., Yang. G.J.J.o.M.C.B., 2014. Chitosan-coated nano-liposomes for the oral delivery of berberine hydrochloride 2(41), 7149–59.
Niu, M., Lu, Y., Hovgaard, L., Guan, P., Tan, Y., Lian, R., et al., Hypoglycemic activity and oral bioavailability of insulin-loaded liposomes containing bile salts in rats: the effect of cholate type, particle size and administered dose. 2012;81(2):265–72.
Niu, M., Tan, Y.n., Guan, P., Hovgaard, L., Lu, Y., Qi, J., et al., 2014. Enhanced oral absorption of insulin-loaded liposomes containing bile salts: a mechanistic study 460 (1-2):119–30.
Nsairat, H., Khater, D., Sayed, U., Odeh, F., Al Bawab, A., Alshaer, W.J.H., 2022. Liposomes: structure, composition, types, and clinical applications 8(5) (2022) e09394.
Park, S.-J., Choi, S.G., Davaa, E., Park, J.-S.J.I.j.o.p., 2011. Encapsulation enhancement and stabilization of insulin in cationic liposomes. 415(1-2), 267-72.
Płaczek, M., Wątróbska-Świetlikowska, D., Stefanowicz-Hajduk, J., Drechsler, M., Ochocka, J.R., Sznitowska, M.J.E.J.o.P.S., 2019. Comparison of the in vitro cytotoxicity among phospholipid-based parenteral drug delivery systems: emulsions, liposomes and aqueous lecithin dispersions (WLDs) 127, 92–101.
Rebolledo-Solleiro, D., Fernández-Guasti, A.J.P., 2018. behavior. Influence of sex and estrous cycle on blood glucose levels, body weight gain, and depressive-like behavior in streptozotocin-induced diabetic rats. 194, 560–7.
Refai, H., Hassan, D., Abdelmonem, R.J.D.d., 2017. Development and characterization of polymer-coated liposomes for vaginal delivery of sildenafil citrate 24(1), 278-88.
Singh, A., Dalal, D., Malik, A.K., Chaudhary, A.J.I.J.M.S.P.H., 2019. Deranged liver function tests in type 2 diabetes: a retrospective study 4(3), 27–31.
Swelum, A.A., El-Saadony, M.T., Abdo, M., Ombarak, R.A., Hussein, E.O., Suliman, G., et al., 2021. Nutritional, antimicrobial and medicinal properties of Camel's milk: a review 28(5), 3126–36.
Thompson, A., Singh, H.J.J.o.D.S., 2006. Preparation of liposomes from milk fat globule membrane phospholipids using a microfluidizer. 89(2):410–9.
van der Veen, J.N., Kennelly, J.P., Wan, S., Vance, J.E., Vance, D.E., Jacobs, R.L.J.B.e.B. A.-B., 2017. The critical role of phosphatidylcholine and phosphatidylethanolamine metabolism in health and disease 1859(9), 1558–72.
Van Hoogevest, P., Wendel, A.J.E.j.o.l.s., technology, 2014. The use of natural and synthetic phospholipids as pharmaceutical excipients 116(9), 1088-107.
Wong, C.Y., Al-Salami, H., Dass, C.R.J.J.o.D.T., 2018. The role of chitosan on oral delivery of peptide-loaded nanoparticle formulation 26(7), 551–62.
Wong, C.Y., Martinez, J., Dass, C.R.J.J.o.P., Pharmacology, 2016. Oral delivery of insulin for treatment of diabetes: status quo, challenges and opportunities 68(9), 1093–108.
Wong, C.Y., Al-Salami, H., Dass, C.R.J.J.o.c.r., 2017 Potential of insulin nanoparticle formulations for oral delivery and diabetes treatment 264, 247–75.
Wong, C.Y., Al-Salami, H., Dass, C.R.J.I.j.o.p., 2018. Recent advancements in oral administration of insulin-loaded liposomal drug delivery systems for diabetes mellitus 549(1-2):201-17.
Yücel, Ç., Altintaş, Y., Değim, Z., Yılmaz, Ş., Arsoy, T., Altıntaş, L., et al., Novel approach to the treatment of diabetes: Embryonic stem cell and insulin-loaded liposomes and nanocochleates. 9(7), 3706–19.